Gain Stabilization and Performance Improvement Induced by a Holding Beam in Semiconductor Optical Amplifiers: Modeling and Experiments

Mrudula Krishna, Govind P Agrawal, *Life Fellow, IEEE*, and Deepa Venkitesh, *Member, IEEE*

***Abstract*—Semiconductor optical amplifiers (SOAs), though available commercially for wideband operation, suffer from nonlinear distortions that become unacceptable for telecom systems operating at high data rates with advanced modulation formats. The use of a holding beam within the SOA's gain spectrum helps in mitigating such distortions. The holding beam saturates the gain, stabilizes it, and reduces fluctuations caused by input signal variations. However, it also leads to a decrease in the signal's gain. We develop a novel heuristic model for SOAs that incorporates the experimentally measurable gain compression and validate it through experiments. Our model offers an effective approach for accurately modeling SOAs as in-line amplifiers.**

***Index Terms*—Assist beam, gain, gain compression, holding beam, Q^2, semiconductor optical amplifier, SOA, SOA model.**

I. Introduction

SEMICONDUCTOR Optical Amplifiers (SOAs) are valued for their small footprint, monolithic integration, and ability to operate over a wide range of wavelengths [1], [2], [3], [4], [5]. Over the past two decades, SOAs have been largely dismissed as in-line amplifiers in telecom systems because of their inferior performance compared to erbium-doped fiber amplifiers (EDFAs), particularly in terms of noise figure, output saturation power, and signal distortion caused by nonlinear gain dynamics. However, SOAs are emerging as strong contenders in specific situations that require wideband amplification, due to their improved performance through band-gap engineering [5].

When an optical signal is launched into an SOA, its amplitude and phase are altered during amplification because of changes in the refractive index resulting from changes in the carrier density. The finite gain recovery time of an SOA resulting from its intrinsic carrier lifetime (around 25 ps), combined with the linewidth enhancement factor and gain saturation, leads to nonlinear distortions in both amplitude and phase when amplifying any time-varying signal with average power close to saturation. When SOAs are used for amplifying high-speed coherent signals with few active channels, a longer gain-recovery time results in poorer performance.

The concept of gain-clamped SOAs has been explored as one way to stabilize the amplifier's gain using an internally generated lasing mode, typically via an integrated or external cavity [6], [7]. An alternative approach to solving this problem employs a secondary continuous-wave (CW) signal, called the holding beam (HB), which is sent into the SOA along with the signal to be amplified. The wavelength of the HB is chosen such that it is well separated from the signal wavelength, but still lies within the bandwidth of the SOA's gain spectrum. The HB's power is made large enough that it is close to the SOA's saturation power. Under these conditions, HB helps stabilize the gain of SOA (by saturating it) and reduce SOA-induced distortions of the signal [5], [8]. The greater the wavelength difference between the HB and the signal, smaller is the gain penalty, but the poorer the ability to compensate for distortions [8]. Similarly, the larger the power of the HB, the faster is the gain recovery time, but the achievable gain [8], [9] becomes smaller. In short, for a given SOA, the wavelength and power of HB determine its performance. Demonstrations with probabilistic-shaped (PS) signals have shown that lower-entropy PS constellations require less HB power to achieve a given performance target than higher-entropy PS or uniform 16QAM signals [10]. Conversely, in a wavelength division multiplexed (WDM) system with many channels, a dedicated HB may be unnecessary because the combined power from adjacent channels can act as a broadband HB [2], [5]. Several experiments have measured the gain compression induced by a HB in both single-channel and few-channel systems [5], [8].

For any device, a mathematical model is necessary to assist in designing and forecasting its performance. Numerous models have been introduced in the past to represent SOAs [11], [12], [13], [14], [15]. The comprehensive wide-band model in [12] is suitable for applications involving the simultaneous amplification of multiple signals at different wavelengths. In [13], a

Received 17 March 2025; revised 19 August 2025; accepted 8 October 2025. Date of publication 14 October 2025; date of current version 16 December 2025. This work was supported by the Ministry of Education, Govt. of India, DST-NSF Pravartak Project, SPARC Project, Govt of India. *(Corresponding author: Deepa Venkitesh.)*

Mrudula Krishna and Deepa Venkitesh are with the Department of Electrical Engineering, Indian Institute of Technology Madras, Chennai 600036, India (e-mail: deepa@ee.iitm.ac.in).

Govind P Agrawal is with The Institute of Optics, University of Rochester, Rochester, NY 14627 USA.

Color versions of one or more figures in this article are available at https://doi.org/10.1109/JLT.2025.3621597.

Digital Object Identifier 10.1109/JLT.2025.3621597

quantum mechanical model is presented considering rear-facet reflections and including a counter-propagating signal. The model in [15] focuses primarily on the gain recovery time of an SOA without including its amplified spontaneous emission (ASE). A comprehensive model is developed in [14] including the impact of ASE-induced gain saturation with emphasis on the self-phase modulation (SPM) phenomenon during amplification of optical pulses. However, existing SOA models do not consider the influence of the HB's wavelength on the signal's gain [12], [13], [14], [15] and cannot be used for optimizing the wavelength and power of a HB, while considering the trade-off between the signal's gain and its distortion.

In this study, we present a heuristic SOA model that incorporates both the empirically observed gain compression induced by a holding beam (HB) and the ASE of the SOA. Some of the initial results were presented in [16], but the model did not account for the ASE of the SOA and relied on a trial-and-error approach to determine the gain compression induced by the HB. In contrast, we introduce here a method for measuring gain compression from a simple measurement of the ASE spectrum of an SOA. We validate the model by comparing simulation results with experimental data. Consequently, this model, along with the ASE spectrum, is sufficient for optimizing the HB parameters required in experiments. Our findings would aid in selecting suitable holding beam parameters for enhancing the performance of SOAs with given design characteristics.

The paper is organized as follows. In Section II, we provide details of our SOA model and define a new parameter, called $Dg_h(\nu_h)$, which accounts for gain compression induced by a HB. The experimental setup is explained in Section III. Section IV presents the experimental validation of the model, where we deduce the value of $Dg_h(\nu_h)$ from the ASE spectrum of the SOA for different power levels and wavelengths of the holding beam. We optimize the HB parameters in Section V for different signal conditions. The main conclusions are summarized in Section VI.

II. Proposed SOA Model

When an optical signal is launched into the SOA, its amplitude and phase change as it propagates through the SOA due to variations in the refractive index, which are caused by changes in the carrier density. To capture the dynamics of carrier density, the time evolution of carrier density $N(z,t)$ of SOA is represented by the following rate (11), (14), (15):

$$\frac{\partial N(z,t)}{\partial t} = \frac{I}{qV} - \frac{N(z,t)}{\tau_c} - g(z,t)\frac{|A_s(z,t)|^2}{h\nu_s} \tag{1}$$

where I is the injected current, q is the electronic charge, V is the volume of active region, τ_c is the carrier lifetime, $g(z,t)$ is the gain coefficient, h is the Planck constant, and ν_s is the signal's frequency. The optical signal is assumed to take the form, $A_s = \sqrt{P_s}e^{j\phi_s}$, where both its power $P_s(z,t)$ and phase $\phi_s(z,t)$ vary with distance z and time t.

Due to electrical pumping, carriers are injected to the conduction band, whose excess density $N(z,t)$ provides optical gain. Considering the so-called lumped model of the SOA [5], [17], the gain coefficient $g(z,t)$ is defined as,

$$g(z,t) = \Gamma a[N(z,t) - N_0]$$

where Γ describes the mode-confinement factor of the active region, a is the differential gain coefficient and N_0 is the carrier density at which the SOA becomes transparent. In the presence of a HB, $A_s(z,t)$ in (1) becomes total input field (HB along with signal). Thus, this model is capable of incorporating the influence of HB's power on the signal's gain. However, it does not account for the fact that signal's gain decreases as the wavelength of HB moves closer to the signal's wavelength, since the gain coefficient in the model described above is assumed to be independent of the wavelength.

To incorporate the gain compression as a function of HB wavelength, we propose to modify (1) as

$$\frac{\partial N(z,t)}{\partial t} = \frac{I}{qV} - \frac{N(z,t)}{\tau_c} - [g(z,t) - dg_h(\nu_h)]\frac{|A(z,t)|^2}{h\nu_s} \tag{2}$$

where $dg_h(\nu_h)$ is the the gain reduction caused by a HB field with instantaneous power $P_h(z,t)$ and phase $\phi_h(z,t)$ at the frequency ν_h. This factor accounts for the gain compression induced by HB and is a function of its frequency. As ν_h moves away from the signal's frequency ν_s, the value of $dg_h(\nu_h)$ decreases, and the signal experiences a higher gain.

By substituting for $N(z,t)$ from Eqn. [II], (2) can be rewritten in terms of $g(z,t)$ as

$$\frac{\partial g(z,t)}{\partial t} = \frac{g_0 - g(z,t)}{\tau_c} - [g(z,t) - dg_h(\nu_h)]\frac{P(z,t)}{E_{sat}} \tag{3}$$

where $E_{sat} = h\nu_s wd/\Gamma a = h\nu_s\sigma/a$ is the saturation energy of SOA, $\sigma = \frac{wd}{\Gamma}$ is the modal cross-sectional area, w is the width of active region, and d is the thickness of active region. The unsaturated gain g_0 depends on injection current I as

$$g_0 = \Gamma a N_0\left(\frac{I}{I_0} - 1\right) \tag{4}$$

where $I_0 = \frac{qVN_0}{\tau_c}$ is the current at which the SOA becomes transparent.

To represent the total gain integrated across the length of SOA, we define a function $h(t)$ such that [11]

$$h(t) = \int_0^L g(z,t)dz \tag{5}$$

The power $P(z,t)$ and phase $\phi(z,t)$ of the signal being amplified evolve inside the SOA as (ignoring its internal loss)

$$\frac{\partial P(z,t)}{\partial z} = [g(z,t) - dg_h(\nu_h)]\,P(z,t) \tag{6}$$

and

$$\frac{\partial \phi(z,t)}{\partial z} = -\frac{1}{2}\alpha_H\,[g(z,t) - dg_h(\nu_h)] \tag{7}$$

where α_H is the linewidth enhancement factor.

We can integrate (7) over the SOA's length to obtain

$$P_{out}(t) = P_{in}(t)\exp\left[h(t) - Dg_h(\nu_h)\right]. \tag{8}$$

where $Dg_h(\nu_h) = \int_0^L dg_h(\nu_h)\, dz$. Similarly the solution to (7) can be written in terms of $h(t)$ as

$$\phi_{out}(t) = \phi_{in}(t) - \frac{1}{2}\alpha_H \left[h(t) - Dg_h(\nu_h)\right]. \tag{9}$$

Integrating (3) over the amplifier's length and eliminating the product $[g(z,t) - dg_h(\nu_h)]P(z,t)$ by using (6), we obtain [11]

$$\frac{\partial h(t)}{\partial t} = \frac{g_0 L}{\tau_c} - \frac{h(t)}{\tau_c} - \frac{1}{E_{sat}}\left[P(L) - P(0)\right] \tag{10}$$

using (8), we can write this equation in terms of P_{in} as

$$\frac{\partial h(t)}{\partial t} = \frac{h_0}{\tau_c} - \frac{h(t)}{\tau_c} - \frac{P_{in}(t)}{P_{sat}\tau_c}\left[e^{h(t)-Dg_h(\nu_h)} - 1\right]. \tag{11}$$

To improve the model, we include internal losses of the SOA through a loss coefficient α and write (6) as

$$\frac{\partial P(z,t)}{\partial z} = [g(z,t) - \alpha - dg_h(\nu_h)]P(z,t). \tag{12}$$

Following the procedure outlined above, (11) becomes

$$\frac{\partial h(t)}{\partial t} = \frac{h_0}{\tau_c} - \frac{h(t)}{\tau_c} - \left[\frac{h(t) - Dg_h(\nu_h)}{h(t) - Dg_h(\nu_h}) - \alpha L\right]$$
$$\frac{P_{in}(t)}{P_{sat}\tau_c}\left(\exp\left[h(t) - Dg_h(\nu_h) - \alpha L\right] - 1\right). \tag{13}$$

Equation (13) is solved using a predictor-corrector method to calculate $h(t)$, which is used to calculate the power and phase at the output end as

$$P_{out}(t) = P_{in}(t)\exp\left[h(t) - Dg_h(\nu_h) - \alpha L\right], \tag{14}$$

$$\phi_{out}(t) = \phi_{in}(t) - \frac{1}{2}\alpha_H\left[h(t) - Dg_h(\nu_h) - \alpha L\right]. \tag{15}$$

To include the effects of carrier heating (CH) and spectral hole burning (SHB), the output field can be rewritten as [5], [18]

$$E_{out}(t) = E_{in}(t)\exp\left(\frac{1}{2}[h(t) - \alpha L - Dg_h(\nu_h)](1 - j\alpha_H)\right.$$
$$\left. + h_{CH}(t)(1 - j\alpha_{CH}) + h_{SHB}(t)\right). \tag{16}$$

where

$$h_{CH}(t) = \frac{-\epsilon_{CH}h(t)P_{in}(t)}{h(t) - Dg_h(\nu_h)} - \alpha L\left[e^{h(t)-Dg_h(\nu_h)} - \alpha L - 1\right] \tag{17}$$

$$h_{SHB}(t) = \frac{-\epsilon_{SHB}h(t)P_{in}(t)}{h(t) - Dg_h(\nu_h)} - \alpha L\left[e^{h(t)-Dg_h(\nu_h)} - \alpha L - 1\right] \tag{18}$$

Here, ϵ_{CH} and ϵ_{SHB} represent the nonlinear gain suppression factors for carrier heating and spectral hole-burning respectively, and α_{CH} stands for gain-phase coupling factor for carrier heating.

To incorporate the effects of ASE, the input signal is combined with white noise, whose power is equivalent to the spontaneous emission power (P_{SE}), calculated as

$$P_{SE} = 2n_{sp}h\nu B, \tag{19}$$

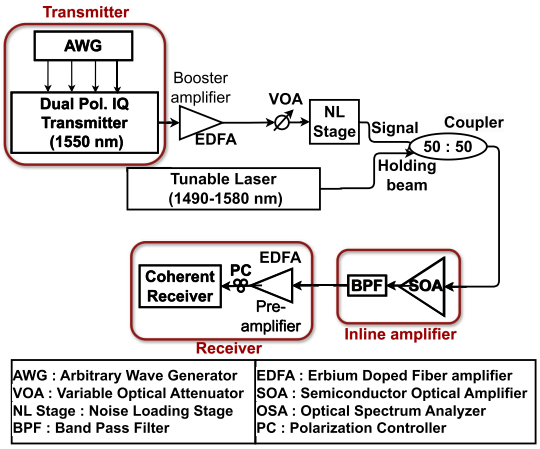

Fig. 1. Schematic for experimentally measuring the gain compression induced by a HB.

where we used $n_{sp} = 3$ for the spontaneous emission factor, $\nu = 193.5$ THz for the central frequency of spontaneous emission, and optical noise bandwidth $B = 8.19$ THz, equal to the simulation bandwidth. Considering this ASE, $P_{in}(t)$ in (13) stands for total power $= P_s(t) + P_h + P_{SE}$. The gain term is excluded in (19) because this noise serves as an input noise to the model. When this noisy input is multiplied by $h(t)$, it yields ASE of the SOA.

III. Experimental Setup

We first measure the gain compression induced by a HB experimentally by performing low-distortion amplification of a single 32-Gbaud 16-QAM channel with our SOA. The setup used for this experiment is shown schematically in Fig. 1. An arbitrary waveform generator (AWG, 23 GHz, 64 GSa/s) produces the desired bit sequence, which is fed into an IQ modulator to obtain 32-Gbaud 16-QAM signal. Both the transmitter and receiver employ low linewidth lasers (25 kHz) centered at 1550 nm. The modulated signal is amplified by an erbium-doped fiber amplifier (EDFA), followed by a variable optical attenuator (VOA) to achieve the desired input signal power of -14 dBm. The VOA output is combined with the output of a noise source at the desired noise power level to emulate an input optical signal-to-noise ratio (OSNR) of 30 dB.

An external-cavity diode laser (tunable from 1490 nm to 1580 nm) serves as the holding beam. Its output is combined with the signal using a 50:50 coupler before being fed into the SOA (Kamelian: SOA-NL-L1-C-FA; polarization dependent gain $<$ 0.5 dB). The SOA used in this study is a quantum well device with an active region length of $\approx$ 1mm. The drive current of the SOA is set to 350 mA to operate in the high gain regime. Its short cavity length and moderate drive requirements may make it suitable for integration in compact subsystems [5]. The output of SOA is passed through a bandpass filter (BPF, 3-dB bandwidth: 1 nm) to filter out the HB. The filtered signal is amplified using a pre-amplifier and sent to a coherent receiver (bandwidth 36 GHz), followed by a real-time oscilloscope (80 GSa/s), which has an optical modulation analyzer (OMA) to

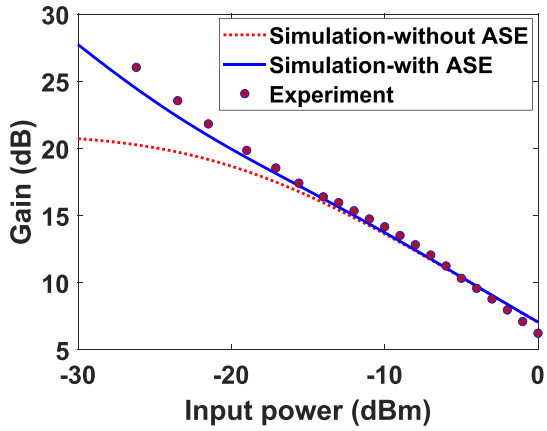

Fig. 2. CW gain for different input power levels (CW signal wavelength = 1550 nm, SOA drive current = 350 mA).

TABLE I
SIMULATION PARAMETERS

Number of symbols	-	2^{15}
Signal wavelength	λ_s	1550 nm
Signal OSNR (before filtering)	-	30 dB
Small signal gain	G_0	21 dB
Saturation power	P_{sat}	1.3 mW
Internal loss	$\alpha_{int}L$	0.004
Carrier life time	τ_s	25 ps
Linewidth enhancement factor	α_L	8
Carrier heating nonlinear gain suppression factor	ϵ_{ch}	$2W^{-1}$
Spectral hole burning nonlinear gain suppression factor	ϵ_{shb}	$1W^{-1}$
Carrier heating gain phase coupling factor	α_{ch}	1
Time resolution	-	122.07 fs
Time window	-	1.024 μs
Frequency resolution	-	976.56 kHz
Frequency window	F_s	8.19 THz

determine performance metrics such as bit error rate (BER), error vector magnitude (EVM) and Q^2 factor. An independent laser source, operating at 1550 nm with an output power of 16 dBm, is used as the local oscillator for the receiver. As signal gain is a function of HB power, the power at the output of BPF (input power to receiver) may vary accordingly. The gain of the pre-amplifier EDFA in the receiver is adjusted to maintain a constant input power at the receiver throughout the experiment, ensuring that any measured noise is solely due to the SOA. Eight data sets are gathered for each trial, and the results (OMA-estimated performance metrics) are averaged for a thorough performance analysis. The gain of the signal and its quality are examined at different HB power levels and wavelengths for further analysis. In our experiments, we define error-free transmission using the HD-FEC BER limit of 10^{-3} . For single-polarization 32 Gbaud 16QAM, this corresponds to an OSNR (0.1 nm bandwidth) of about 18 dB and a Q^2 factor of $\approx$ 9.79 dB at a received signal power of + 4 dBm in our coherent receiver.

IV. EXPERIMENTAL VALIDATION OF THE MODEL

In this section, the SOA model proposed in Section II is validated by comparing the simulation results with experimental data. To solve the (13) in MATLAB and obtain the output SOA field as described in (16), it is essential to have accurate information about the small-signal gain coefficient ($h_0 = g_0 L$) and saturation power P_{sat} of the SOA used in the experiment. Parameters such as carrier lifetime (τ_c) and intrinsic SOA loss (αL) are known from the SOA datasheet.

A. Determination of Small-Signal Gain and Saturation Power

To measure the gain coefficient h_0 and saturation power P_{sat}, a CW signal is sent through the SOA (drive current: 350 mA), and input and output signal powers are monitored using a power meter. The gain as a function of input signal power is measured experimentally, and the results are shown in Fig. 2. The small-signal gain coefficient g_0 and the saturation power P_{sat} are found by fitting the experimental data to the (11),

$$G = \exp\left[\frac{g_0}{1 + \frac{P_{in}}{P_{sat}}}\right], \tag{20}$$

where G represents the power gain at a specific input power P_{in}. After fitting the experimental data, the small-signal gain ($G_0 = e^{h_0} = e^{g_0 L}$) is found to be 21 dB (small signal material gain per unit length, $g_0(z) = 48.354\ \text{cm}^{-1}$) with a saturation power (P_{sat}) of 1.3 mW. These parameters are utilized in simulations to accurately model the gain saturation in our SOA. To validate the model for gain-saturation effects, $Dg_h(\nu_h)$ is set to 0, as the experiment was conducted without the HB. Other simulation parameters are listed in Table I. In Fig. 2, the experimental data (circles) is compared with the simulation results in two cases. The solid blue line represents results with ASE, while the dotted red line shows results without ASE. The over estimation of gain in the low input power region (small-signal regime) is due to ASE contributions.

B. Signal Gain at a Fixed HB Wavelength

First, amplification of a 32-Gbaud 16-QAM signal (average power = -14 dBm) is carried out by the SOA without a HB (tunable laser is turned off) using the setup in Fig. 1. The corresponding simulation results are also obtained by setting $Dg_h(\nu_h)$ to 0 with the parameters given in Table I. The signal gain in the absence of a HB is found to be $\approx$ 16 dB both through simulation and experiments, validating the efficacy of the model for comparison with the experiments.

As a next step, the tunable laser (see Fig. 1) is turned on, and the HB wavelength is set to 1510 nm. Amplification of the 32-Gbaud low-power data is carried out as the HB power is varied from 0.1 to 1 mW. The Red circles in Fig. 3 show the experimental results. The solid blue line shows the results of numerical simulations when $Dg_h(\nu_h)$ is set to -0.66. The rationale for selecting this value is discussed in the next section. The excellent agreement seen in Fig. 3 also justifies this value. As anticipated, the signal gain decreases with increasing HB power. It can be inferred from Fig. 3 that $Dg_h(\nu_h)$ remains

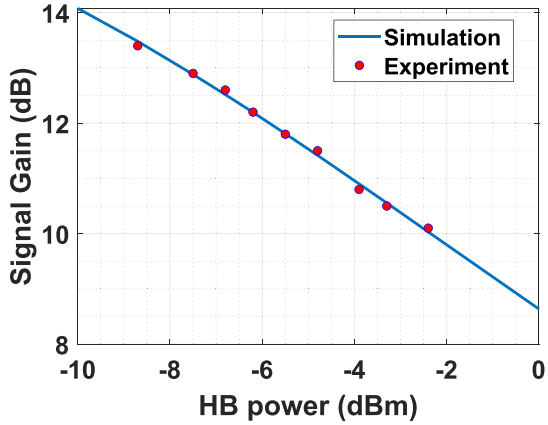

Fig. 3. Signal gain as a function of HB power (Signal wavelength = 1550 nm, SOA drive current = 350 mA).

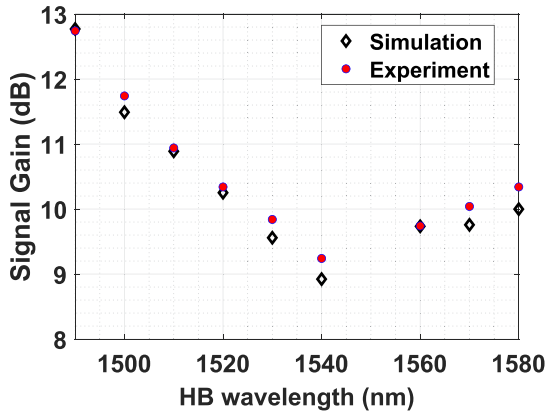

Fig. 4. Signal gain as a function of HB wavelength (Signal wavelength = 1550 nm, SOA drive current = 350 mA).

constant with varying HB power, provided the HB wavelength is fixed.

C. Signal Gain at Different HB Wavelengths

To analyze the variation of $Dg_h(\nu_h)$ with changes in HB wavelength, the same 32-Gbaud 16-QAM signal (average power $= -14$ dBm) is amplified using an SOA (driven at 350 mA) in the presence of an HB whose power is kept constant at -4 dBm while wavelength is varied from 1490 to 1580 nm. The experimental results for the signal gain in this wavelength range are shown by red circles in Fig. 4. The gain decreases initially, becomes minimum near the 1540-nm wavelength, and increase afterward. Clearly, the gain compression induced by a HB depends on its wavelength. Knowledge of this dependence is essential for numerical simulations.

We have identified that the wavelength dependence of $Dg_h(\nu_h)$ can be inferred from the ASE spectrum of our SOA. We discuss this approach in the next subsection. Here we show that this approach fits the data shown in Fig. 4 reasonably well. The computed values of signal gain as a function of the HB wavelength are shown by black triangles in Fig. 4.

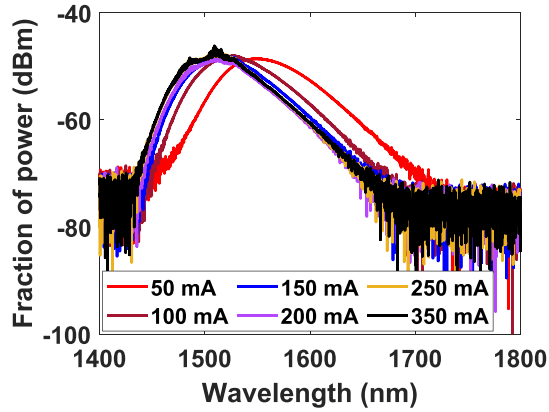

Fig. 5. ASE (forward) spectrum as a function of SOA drive current.

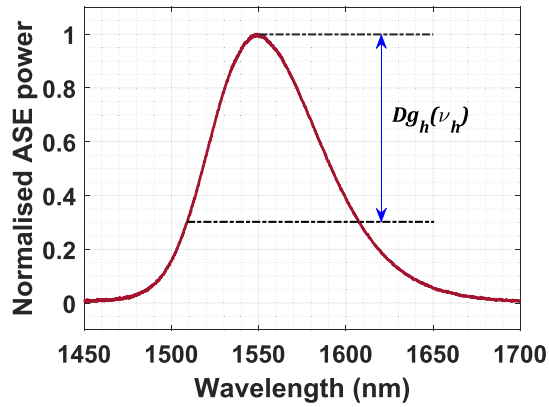

Fig. 6. Estimating Dg_h from ASE spectrum.

D. Estimation of $Dg_h(\nu_h)$ Using ASE Spectrum

We measured the forward ASE spectrum at different SOA drive currents, and the results are shown in Fig. 5. It is observed that the peak wavelength exhibits a blue shift with increasing drive current. Additionally, the SOA begins to lase at high drive currents, but no lasing is detected at 50 mA. From the ASE spectrum at 50 mA, normalized to 1 at its peak, $Dg_h(\nu_h)$ can be estimated as the difference between its values at the signal wavelength and at the HB wavelength, as illustrated in Fig. 6. The ASE spectrum at 50 mA is preferred for this estimation because the SOA remains in a non-lasing state.

The $Dg_h(\nu_h)$ values obtained with this method are shown by blue squares in Fig. 7 and are found to be in close agreement with those derived from the trial-and-error method. Additionally, the maroon diamonds in Fig. 7 represent the estimated $Dg_h(\nu_h)$ values obtained using the backward ASE spectrum, instead of the forward ASE spectrum. A comparison indicates that there is no significant difference in the $Dg_h(\nu_h)$ values derived from the forward and backward ASE spectra. Thus, the $Dg_h(\nu_h)$ value can be reliably determined using either the forward or backward ASE spectrum at a low drive current where lasing does not occur. The black diamonds in Fig. 4 represent the simulation results obtained using the $Dg_h(\nu_h)$ values derived from the forward ASE spectrum (blue squares in Fig. 7). All other simulation parameters remain unchanged, as specified in

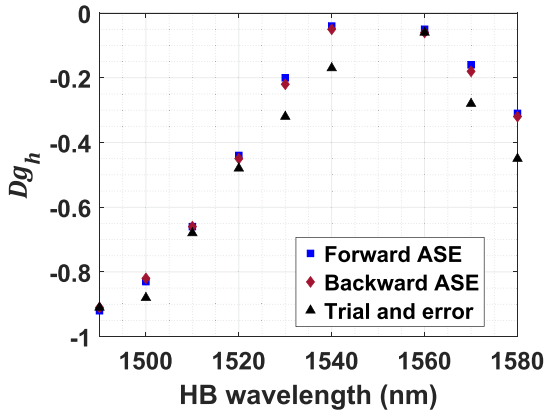

Fig. 7. Dg_h as a function of input HB wavelength (signal wavelength = 1550 nm).

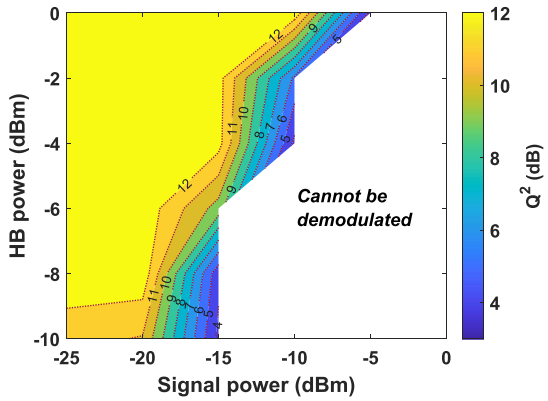

Fig. 9. Simulation results for SP 32-GBaud 16 QAM : Q^2 as a function of signal and holding beam powers ($\nu_h = 1510$ nm, $\nu_s = 1550$ nm).

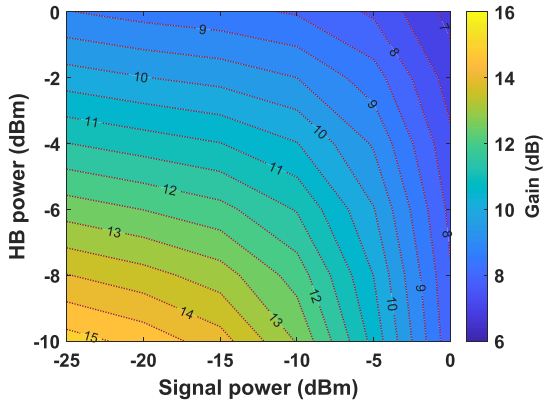

Fig. 8. Signal-gain contours as a function of signal and holding beam powers ($\nu_h = 1510$ nm, $\nu_s = 1550$ nm).

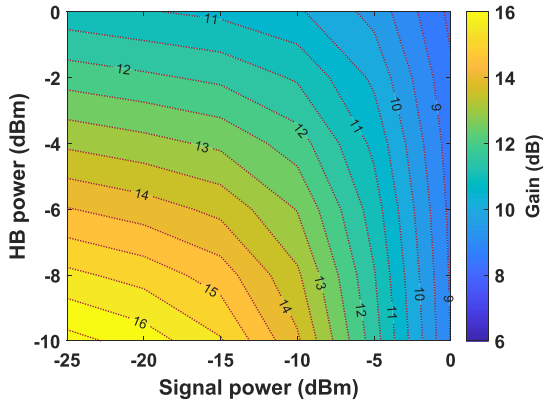

Fig. 10. Signal gain as a function of signal and holding beam power ($\nu_h = 1490$ nm, $\nu_s = 1550$ nm).

Table I. Fig. 4 demonstrates that the simulated signal gain closely corresponds with the experimental results, indicating that the model effectively replicates gain compression (and signal gain) as a function of the HB wavelength.

V. Optimization of the Holding Beam Parameters

Our earlier work demonstrated that increasing the HB power improves the BER (i.e., signal quality) by reducing SOA-induced distortions, albeit at the cost of a reduction in signal gain [8]. Furthermore, both the signal gain and quality are influenced by the HB wavelength. Utilizing the proposed model, we analyze this trade-off to determine the optimized HB parameters for given operating conditions.

To assess the quality of the 32-Gbaud 16-QAM signal after the SOA, we calculate the Q^2 factor of the amplified signal in the presence of HB. Figs. 8 and 9 show variations in the gain and Q^2 as functions of signal power (at 1550 nm) and HB power (at 1510 nm). Fig. 8 indicates that signal gain decreases with increasing HB power and signal power. Conversely, Fig. 9 shows that signal quality improves with increasing HB power for a given signal power. Additionally, Fig. 9 highlights a region where the signal becomes so distorted that its demodulation becomes infeasible.

By comparing Figs. 8 and 9, it is evident that increasing HB power results in gain reduction while improving the Q^2 factor. Notably, a HB with -4 dBm power provides a better trade-off, offering improved signal quality with a relatively high gain compared to a HB with 1 mW power (0 dBm). If a higher HB power is used, the gain reduction becomes quite significant, while the Q^2 improvement remains minimal. Therefore, the former is a practical choice, as it provides sufficient Q^2 enhancement, while minimizing the reduction in gain.

To optimize the HB wavelength, we conducted simulations for a HB with a wavelength of 1490 nm. Figs. 10 and 11 present the variations in gain and Q^2 as functions of signal power (32-Gbaud 16-QAM at 1550 nm) and HB power (at 1490 nm). A comparison between Figs. 8 and 10 reveals that the use of a shorter wavelength results in an increase in signal's gain for a given combination of the signal and HB power levels. Similarly, a comparison of Figs. 9 and 11 indicates that a longer HB wavelength enhances signal's quality for the same signal and HB power levels. Specifically, with a -4 dBm HB power at 1510 nm, a 32-Gbaud 16-QAM signal at 1550 nm with -15 dBm input power achieves a gain of 11 dB with a Q^2 of around 12 dB.

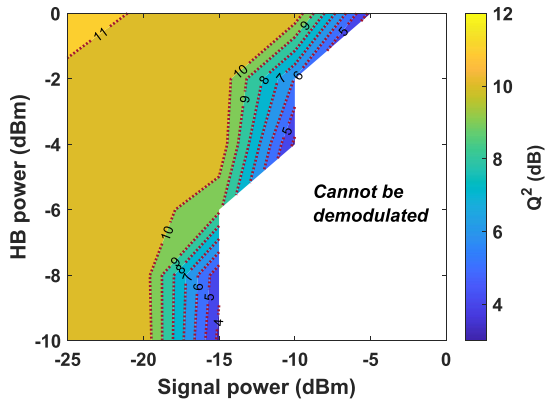

Fig. 11. Simulation results for SP 32-GBaud 16 QAM : Q^2 as a function of signal and holding beam power ($\nu_h = 1490$ nm, $\nu_s = 1550$ nm).

VI. Conclusion

A novel heuristic model for SOA is proposed to characterize the gain stabilization induced by a holding beam. The accuracy of the model is validated by comparing simulation results with experimental data. Additionally, the ASE spectrum at low SOA drive currents is utilized to estimate $Dg_h(\nu_h)$ as a function of the HB wavelength. Our experiments and numerical simulations reveal the optimal power and wavelength of the holding beam for a 32-Gbaud 16-QAM signal at 1550 nm. Specifically, we found that a relatively low (-4 dBm) power of the holding beam at 1510 nm provides a gain of 11 dB and a Q^2 of around 12 dB for a 32-Gbaud 16-QAM signal at 1550 nm launched into our SOA with -15 dBm input power. Our model should prove useful for optimizing telecom channels operating at different wavelengths and power levels.

References

[1] A. Arnould et al., "Impact of the number of channels on the induced nonlinear distortions in ultra-wideband SOAs," in *Proc. Opt. Fiber Commun. Conf. Exhib. (OFC)*, 2019, pp. 1–3.

[2] J. Renaudier et al., "Recent advances in 100 nm ultra-wideband fiber-optic transmission systems using semiconductor optical amplifiers," *J. Lightw. Technol.*, vol. 38, no. 5, pp. 1071–1079, Mar. 2020.

[3] S. Murthy et al., "Large-scale photonic integrated circuit transmitters with monolithically integrated semiconductor optical amplifiers," in *Proc. Conf. Opt. Fiber Commun./National Fiber Optic Engineers Conf.*, 2008, pp. 1–3.

[4] T. Matsumoto et al., "Hybrid-integration of SOA on silicon photonics platform based on flip-chip bonding," *J. Lightw. Technol.*, vol. 37, no. 2, pp. 307–313, Jan. 2019.

[5] A. Sobhanan et al., "Semiconductor optical amplifiers: Recent advances and applications," *Adv. Opt. Photon.*, vol. 14, pp. 571–651, 2022.

[6] D. Wolfson, "Detailed theoretical investigation and comparison of the cascadability of conventional and gain-clamped SOA gates in multiwavelength optical networks," *IEEE Photon. Technol. Lett.*, vol. 11, no. 11, pp. 1494–1496, Nov. 1999.

[7] G. Giuliani and D. D'Alessandro, "Noise analysis of conventional and gain-clamped semiconductor optical amplifiers," *J. Lightw. Technol.*, vol. 18, pp. 1256–1263, Sep. 2000.

[8] M. Krishna and D. Venkitesh, "Low distortion inline SOA amplifier with optimized holding beam for single-channel 16/64QAM signals," *IEEE Photon. Technol. Lett.*, vol. 36, no. 13, pp. 845–848, Jul. 2024.

[9] Y. Ben-Ezra, B. I. Lembrikov, and M. Haridim, "Acceleration of gain recovery and dynamics of electrons in QD-SOA," *IEEE J. Quantum Electron.*, vol. 41, no. 10, pp. 1268–1273, Oct. 2005.

[10] S. A. Mir, M. Krishna, and D. Venkitesh, "Low-distortion amplification of probabilistic shaped signals using SOA," *IEEE Photon. Technol. Lett.*, vol. 36, no. 14, pp. 897–900, Jul. 2024.

[11] G. P. Agrawal and N. A. Olsson, "Self-phase modulation and spectral broadening of optical pulses in semiconductor laser amplifiers," *IEEE J. Quantum Electron.*, vol. 25, pp. 2297–2306, Nov. 1989.

[12] M. Connelly, "Wideband semiconductor optical amplifier steady-state numerical model," *IEEE J. Quantum Electron.*, vol. 37, no. 3, pp. 439–447, Mar. 2001.

[13] K. S. Anzabi, A. Habibzadeh-Sharif, M. J. Connelly, and A. Rostami, "Wideband steady-state and pulse propagation modeling of a reflective quantum-dot semiconductor optical amplifier," *J. Lightw. Technol.*, vol. 38, no. 4, pp. 797–803, Feb. 2020.

[14] P. P. Baveja, D. N. Maywar, A. M. Kaplan, and G. P. Agrawal, "Self-phase modulation in semiconductor optical amplifiers: Impact of amplified spontaneous emission," *IEEE J. Quantum Electron.*, vol. 46, no. 9, pp. 1396–1403, Sep. 2010.

[15] M. Krishna, A. Sobhanan, and D. Venkitesh, "Numerical studies on the estimation of carrier lifetime of SOAs from gain-recovery time measurements," in *Proc. Opt. Compon. Mater. XVIII*, Bellingham, WA, USA: SPIE, 2021, vol. 11682, pp. 1–8.

[16] M. Krishna, G. P. Agrawal, and D. Venkitesh, "Gain compression in semiconductor optical amplifiers induced by a holding beam," in *Proc. IEEE Photon. Conf. (IPC)*, 2024, pp. 1–2.

[17] S. O Duill and L. Barry, "Improved reduced models for single-pass and reflective semiconductor optical amplifiers," *Opt. Commun.*, vol. 334, pp. 170–173, 2015.

[18] A. Mecozzi and J. Mørk, "Saturation effects in nondegenerate four-wave mixing between short optical pulses in semiconductor laser amplifiers," *IEEE J. Sel. Topics Quantum Electron.*, vol. 3, no. 5, pp. 1190–1207, Oct. 1997.